Electronic Supplementary Material (ESI) for Journal of Materials Chemistry A.

Supporting Information

Tuning the Electrochemical Behavior of Organodisulfides in Rechargeable Lithium Batteries by N-Containing Heterocycles

Dan-Yang Wang,[a] Yubing Si,*[b] Junjie Li,[c] and Yongzhu Fu*[a]

[a] College of Chemistry and Molecular Engineering, Zhengzhou University, Zhengzhou 450001, P. R. China

[b] Henan Provincial Key Laboratory of Nanocomposites and Applications, Institute of Nanostructured Functional Materials, Huanghe Science and Technology University, Zhengzhou 450006, P. R. China

[c] Research Technologies, Indiana University, Indianapolis, IN 46202, U. S. A.

Experimental Section:

Materials: Commercial lithium-sulfur electrolyte (1.0 M LiTFSI in DOL:DME =1:1 vol% with 1.0% $LiNO_3$), and 2,2'-dipyridyl disulfides (2,2'-DpyDS, $C_5H_4NSSC_5H_4N$, 98%), 4,4'-dipyridyl disulfides (4,4'-DpyDS, $C_5H_4NSSC_5H_4N$, 98%), dipyridyl disulfide-N,N'-dioxide (DpyDSDO, $C_5H_4NOSSC_5H_4NO$, 98%) were purchased and used as received.

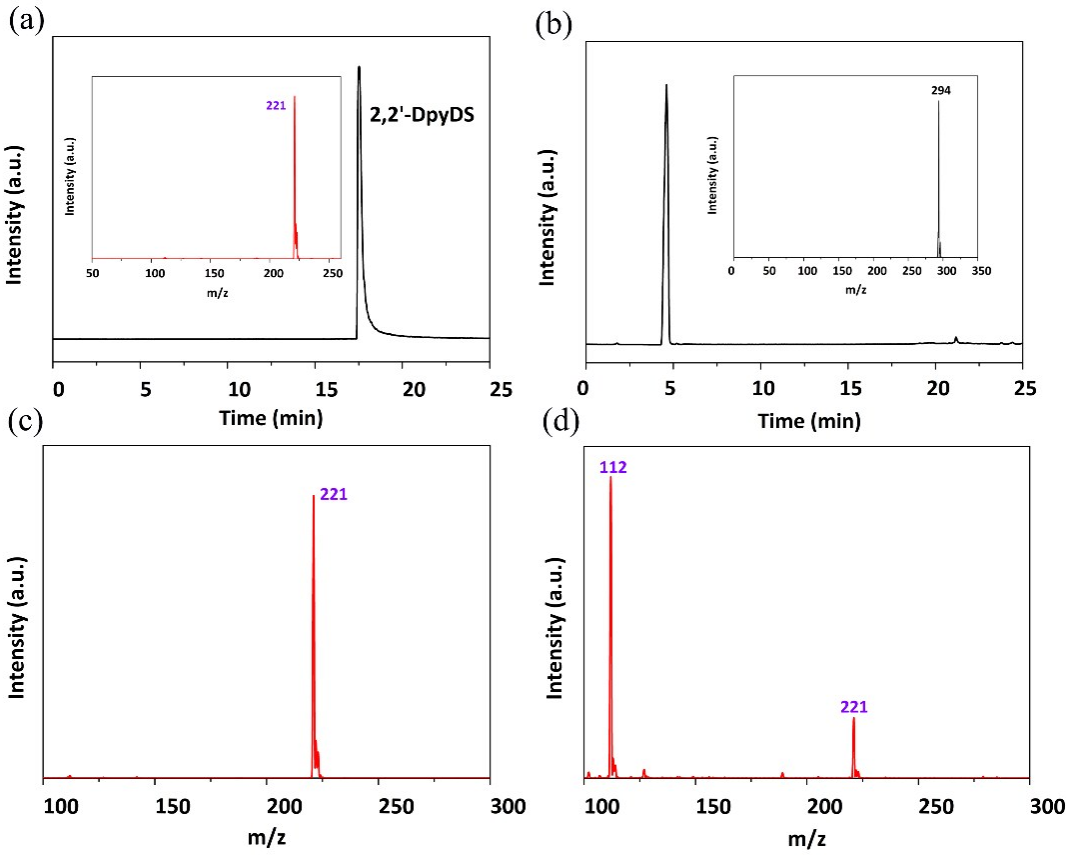

Figure S1. Liquid chromatogram and mass spectrum of 2,2'-DpyDS (a) and the electrolyte (b); mass spectra of **c** peak (c) and **a** peak (d) from the 2,2'-DpyDS electrode after recharge.

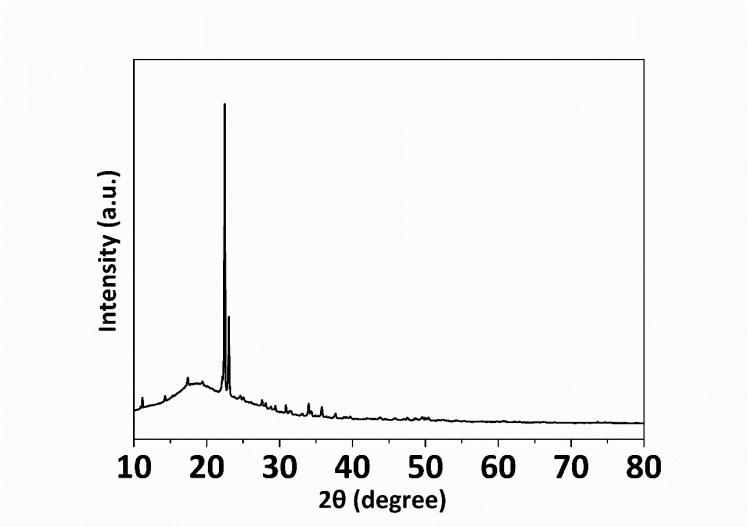

Figure S2. X-ray diffractogram of commercial 2,2'-DpyDS.

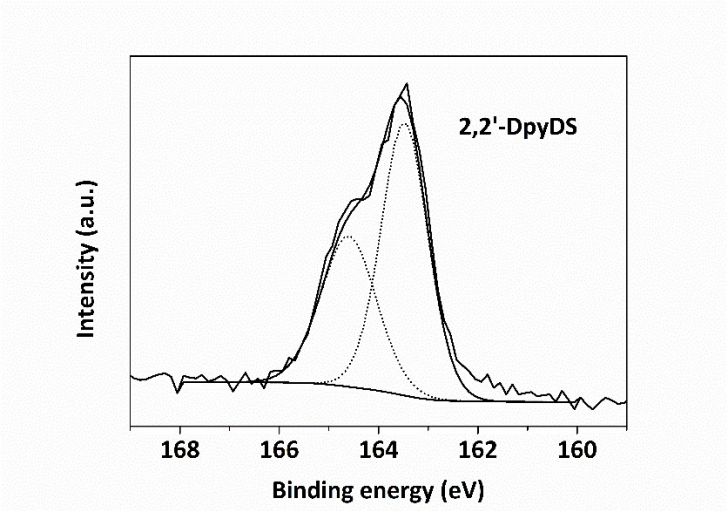

Figure S3. XPS spectrum of sulfur 2p of 2,2'-DpyDS.

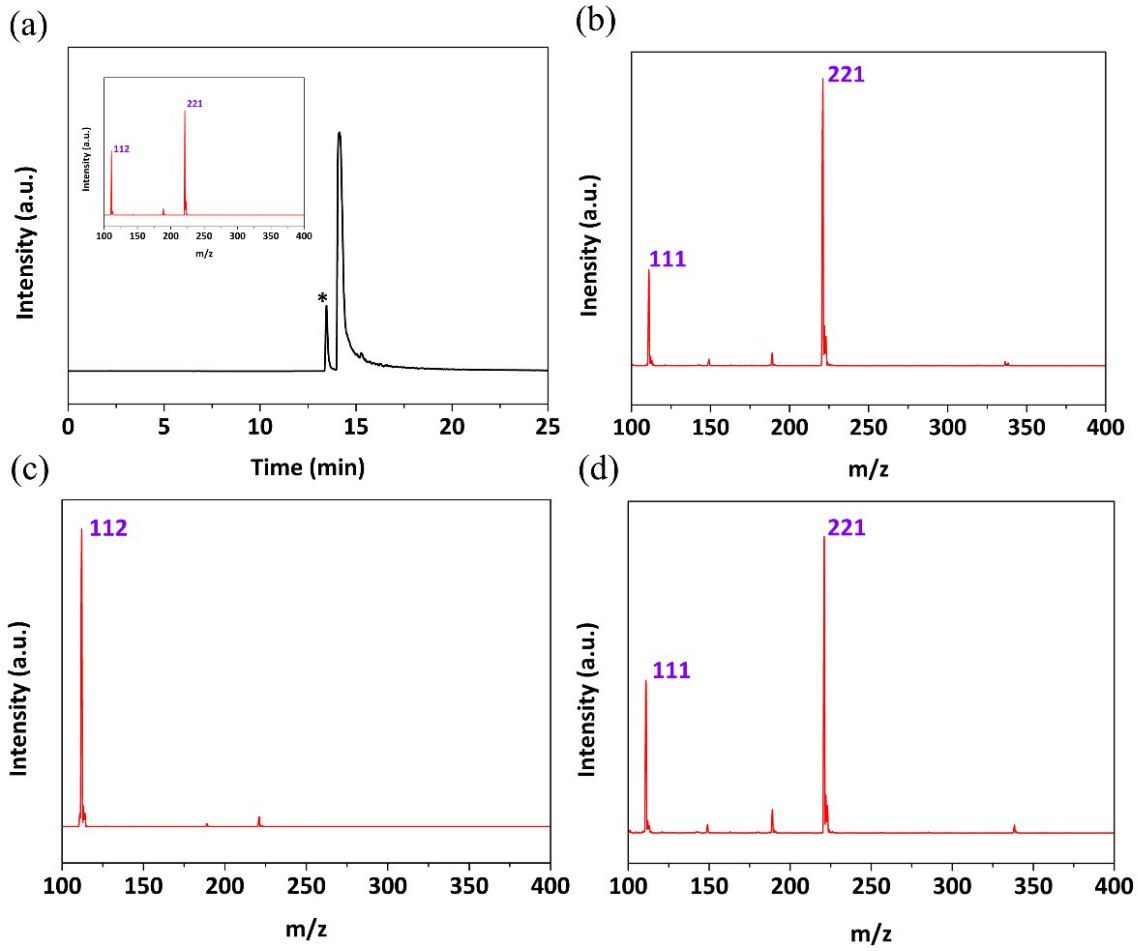

Figure S4. (a) Liquid chromatogram and mass spectrum of 4,4'-DpyDS; mass spectra of **f** peak (b) and **d** peak (c) from the 4,4'-DpyDS electrode after discharge; (d) mass spectrum of **f** peak from the 4,4'-DpyDS electrode after recharge.

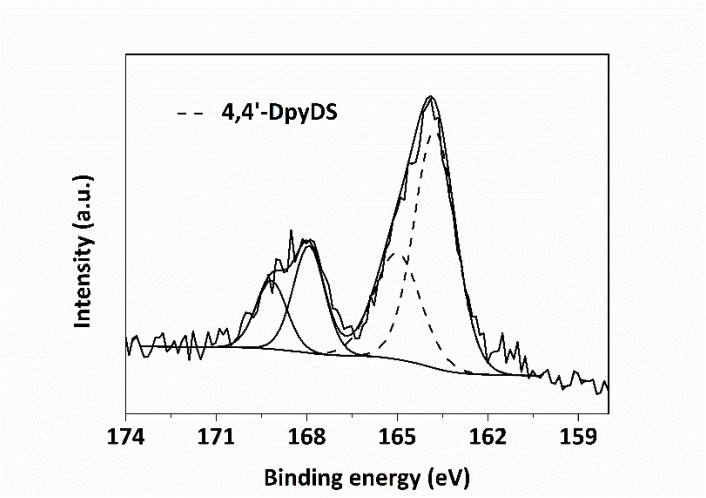

Figure S5. XPS spectrum of sulfur 2p of 4,4'-DpyDS.

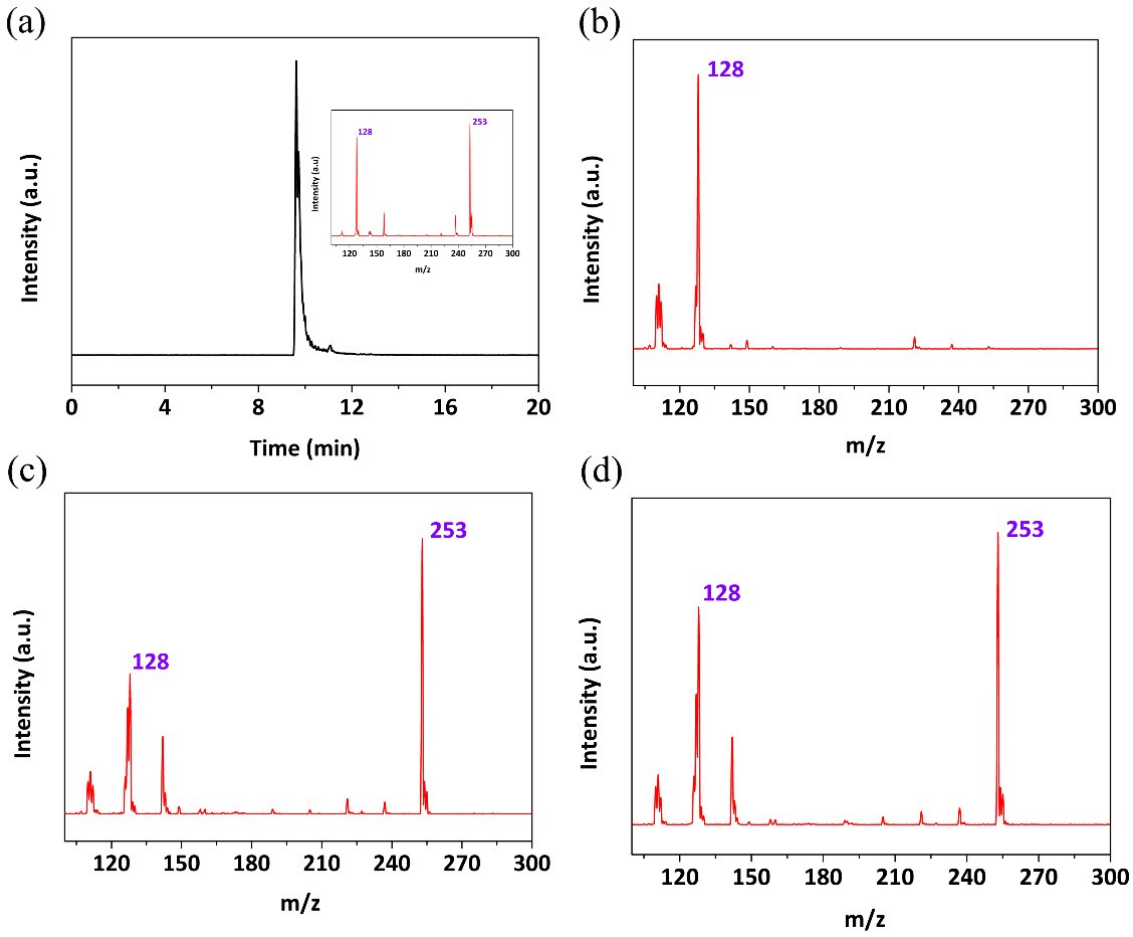

Figure S6. (a) Liquid chromatogram and mass spectrum of DpyDSDO; mass spectra of **g** peak (b) and **i** peak (c) from the DpyDSO electrode after discharge; (d) mass spectrum of **i** peak from the DpyDSO electrode after recharge.

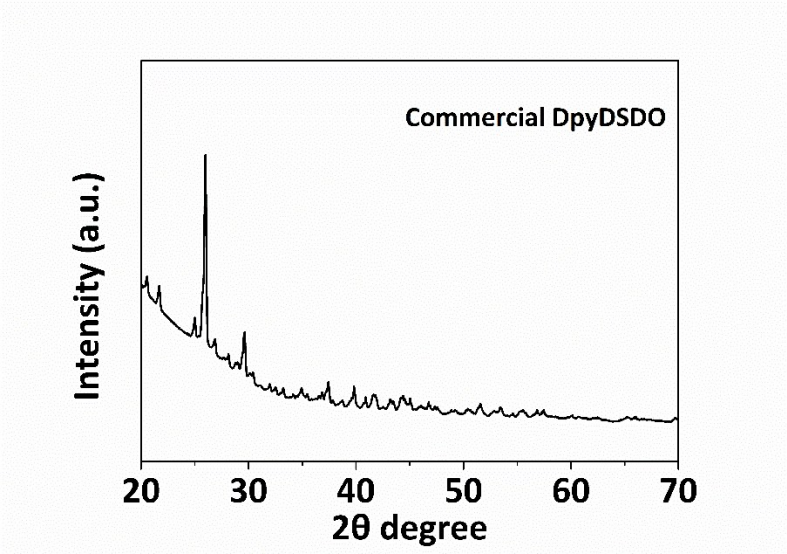

Figure S7. X-ray diffractogram of commercial DpyDSDO.

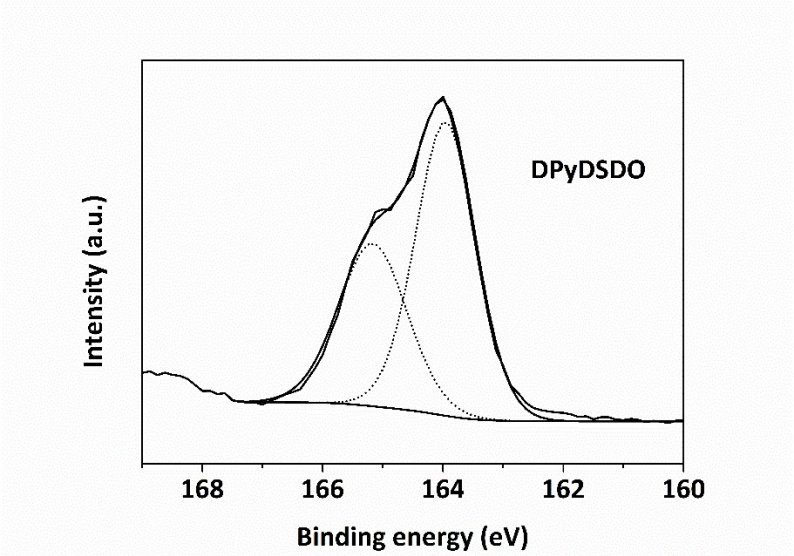

Figure S8. XPS spectrum of sulfur 2p of DpyDSDO.

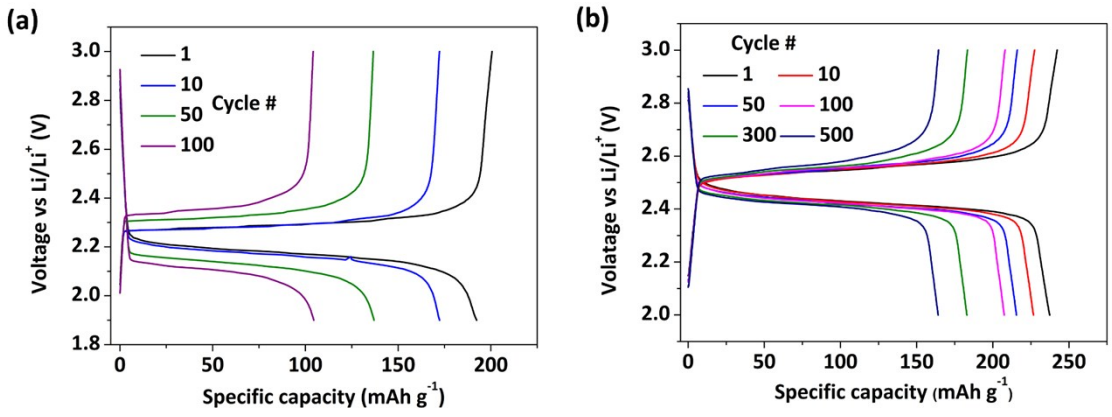

Figure S9. (a) The voltage-capacity profiles of the Li/DPDS cell at C/2 rate in different cycles; (b) the voltage-capacity profiles of the Li/2,2'-DpyDS cell at C/2 rate in different cycles

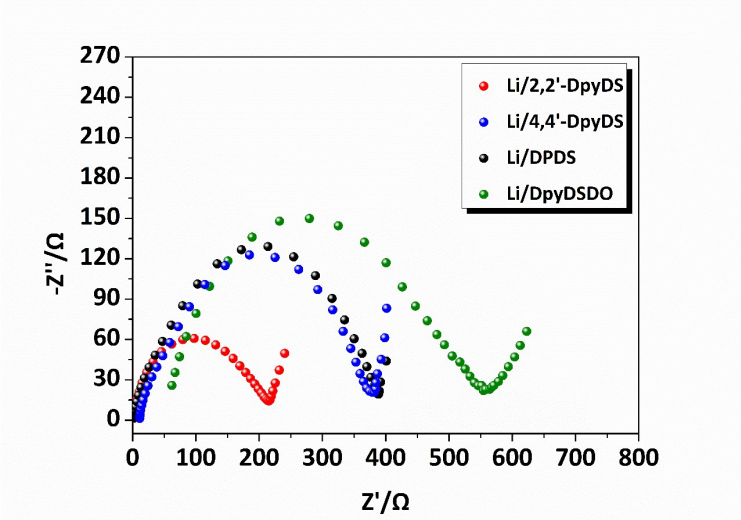

Figure S10. Impedance spectra of Li/2,2'-DpyDS, Li/4,4'-DpyDS, Li/DPDS, and Li/DpyDSDO cells.

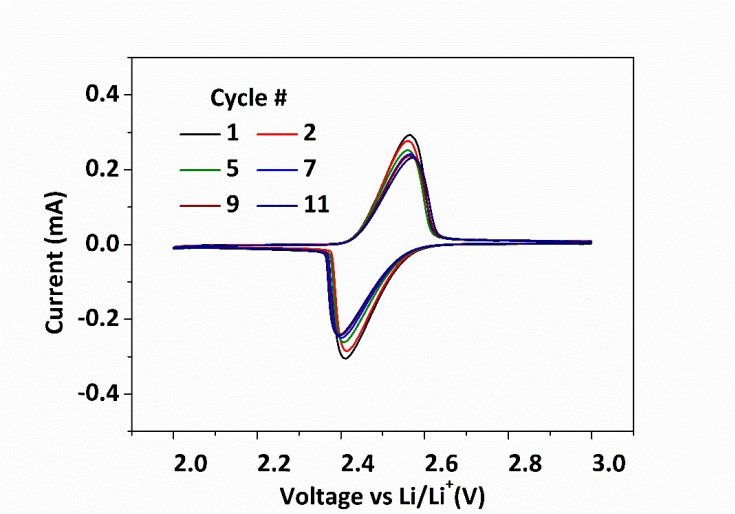

Figure S11. Selected cyclic voltammograms of the Li/2,2'-DpyDS cell performed at a scan rate of 0.05 mV s^{-1}.

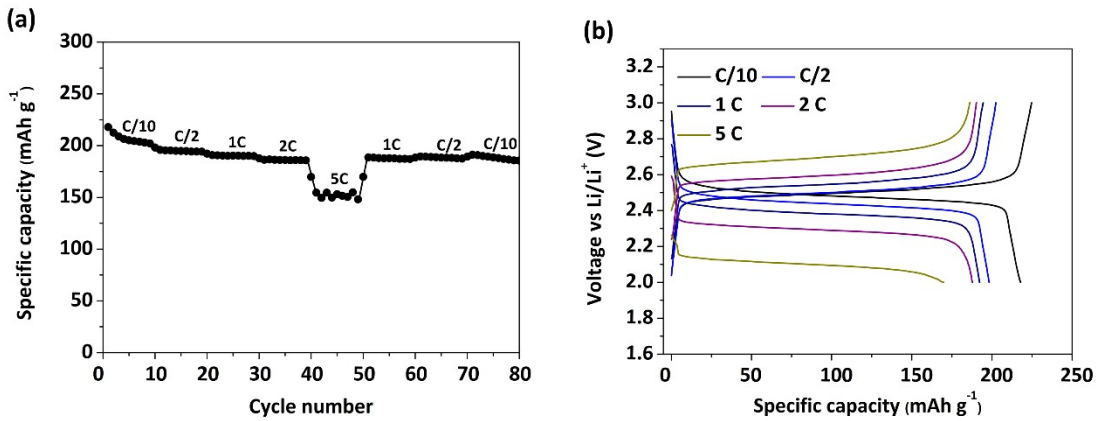

Figure S12. (a) Rate performance of the Li/2,2'-DpyDS cell; (b) selected voltage-capacity profiles at different C rates.

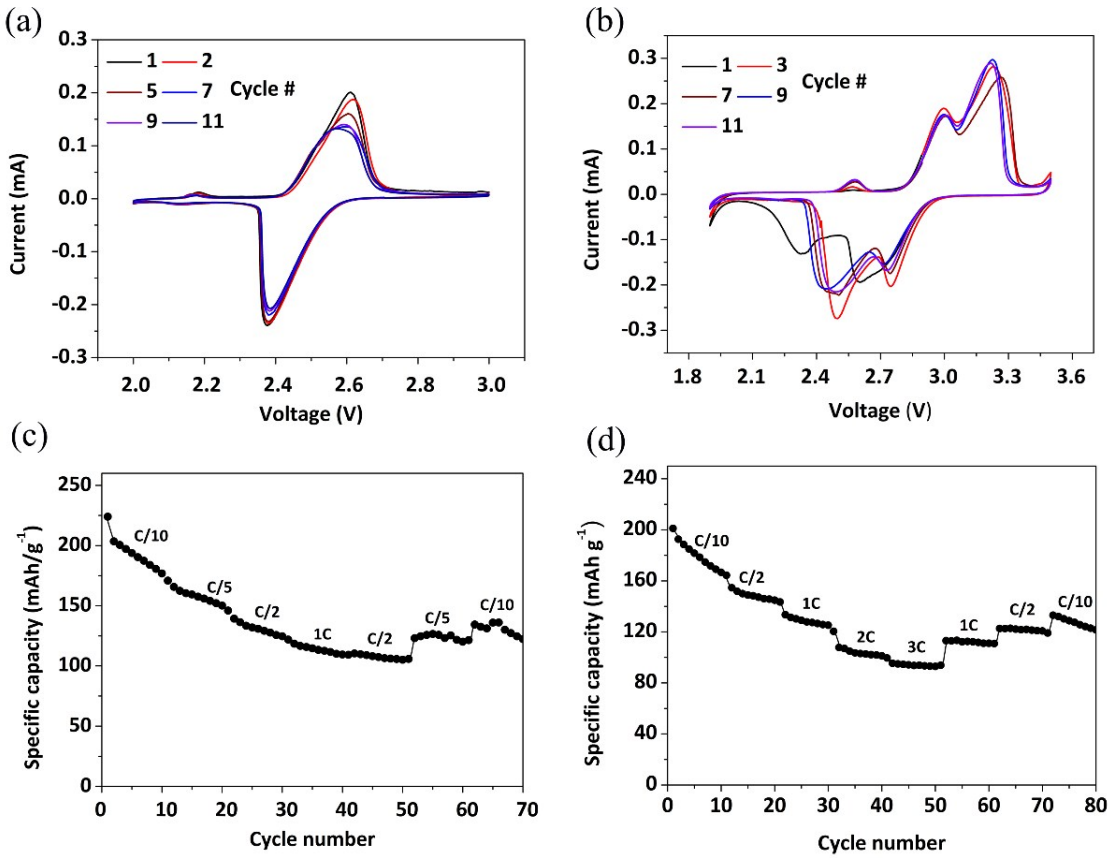

Figure S13. Selected cyclic voltammograms of the Li/4,4'-DpyDS cell (a) and Li/DpyDSO cell (b) performed at a scan rate of 0.05 mV s^{-1}; rate performance of the Li/4,4'-DpyDS cell (c) and Li/DpyDSO cell (d).

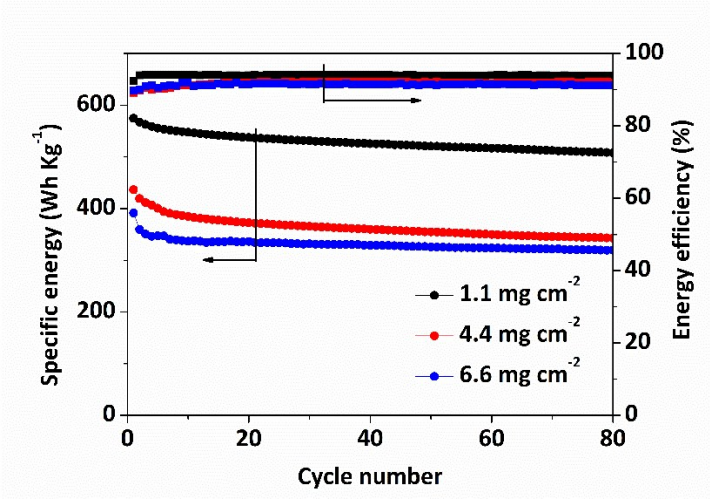

Figure S14. Specific energies of 2,2'-DpyDS in lithium cells with different mass loadings at C/2 rate.

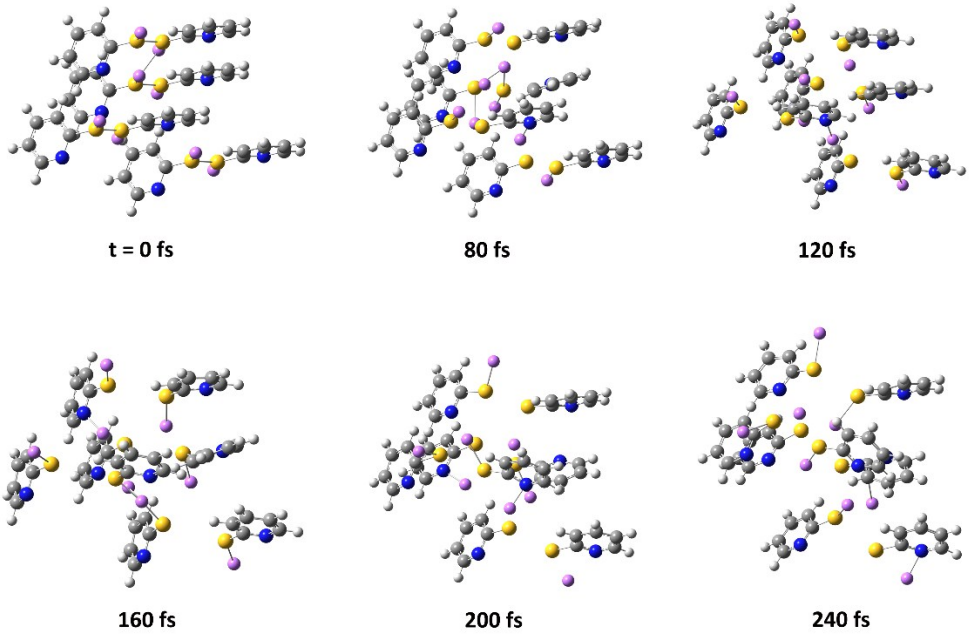

Figure S15. Six typical snapshots along the BOMD trajectory of 2,2-DpyDS and the corresponding time evolution of the potential energy.

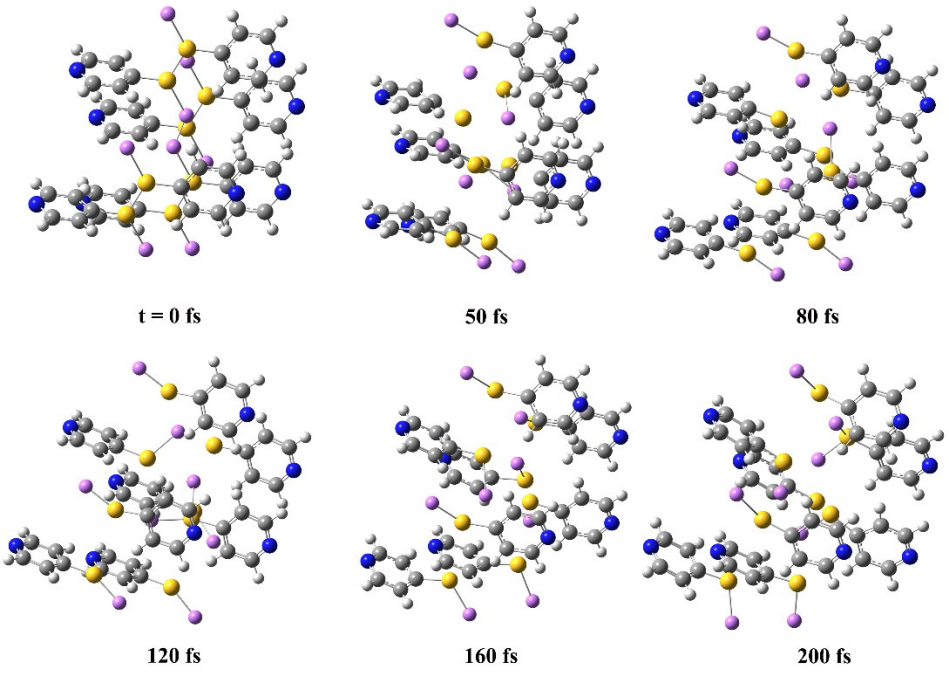

Figure S16. Six typical snapshots along the BOMD trajectory of 4,4-DpyDS and the corresponding time evolution of the potential energy.